Quantitative low-dose rest and stress CT myocardial perfusion imaging with a whole-heart coverage scanner improves functional assessment of coronary artery disease

I-Lun Huang [a,b,1], Ming-Ting Wu [a,b,1], Chin Hu [c], Guang-Yuan Mar [d], Ting-Yim Lee [e,f], Aaron So [f,*]

[a] Radiology, Kaohsiung Veteran General Hospital, Kaohsiung, Taiwan
[b] Faculty of Medicine, School of Medicine, National Yang Ming University, Taipei, Taiwan
[c] Nuclear Medicine, Kaohsiung Veteran General Hospital, Kaohsiung, Taiwan
[d] Cardiology, Kaohsiung Veteran General Hospital, Kaohsiung, Taiwan
[e] Imaging, Robarts Research Institute, London, Ontario, Canada
[f] Imaging, Lawson Health Research Institute, London, Ontario, Canada

ARTICLE INFO

ABSTRACT

Objective: We evaluated the diagnostic accuracy of myocardial blood flow (MBF) and perfusion reserve (MPR) measured from low-dose dynamic contrast-enhanced (DCE) imaging with a whole-heart coverage CT scanner for detecting functionally significant coronary artery disease (CAD).

Methods: Twenty one patients with suspected or known CAD had rest and dipyridamole stress MBF measurements with CT and SPECT myocardial perfusion imaging (MPI), and lumen narrowing assessment with coronary angiography (catheter and/or CT based) within 6 weeks. SPECT MBF measurements and coronary angiography were used together as reference to determine the functional significance of coronary artery stenosis. In each CT MPI study, DCE images of the whole heart were acquired with breath-hold using a low-dose acquisition protocol to generate MBF maps. Binomial logistic regression analysis was used to determine the diagnostic accuracy of CT-measured MBF and MPR (ratio of stress to rest MBF) for assessing functionally significant coronary stenosis.

Results: Mean stress MBF and MPR in ischemic segments were lower than those in non-ischemic segments (1.37 ± 0.34 vs. 2.14 ± 0.64 ml/min/g; 1.56 ± 0.41 vs. 2.53 ± 0.70; $p < 0.05$ for all). The receiver operating characteristic curve analysis revealed that MPR (AUC 0.916, 95%CI: 0.885–0.947) had a superior power than stress MBF (AUC 0.869, 95%CI: 0.830–0.909) for differentiating non-ischemic and ischemic myocardial segments ($p = 0.045$). On a per-vessel and per-segment analysis, concomitant use of MPR and stress MBF thresholds further improved the diagnostic accuracy compared to MPR or stress MBF alone for detecting obstructive coronary lesions (per-vessel: 93.4% vs. 83.6% and 88.5%, respectively; per-segment: 90.0% vs. 83.7% and 83.1%, respectively). The estimated effective dose of a rest and stress CT MPI study was 3.04 and 3.19 mSv respectively.

Conclusion: Quantitative rest and stress myocardial perfusion measurement with a large-coverage CT scanner improves the diagnostic accuracy for detecting functionally significant coronary stenosis.

1. Introduction

Myocardial perfusion reserve (MPR), conventionally known as coronary flow reserve, is the theoretical gold standard for assessing myocardial ischemia in coronary artery disease (CAD) and also a powerful prognostic factor [1]. CT Perfusion (CTP) can measure MPR through imaging the first-pass distribution of iodinated contrast in the myocardium, but the measurement can be affected by excessive image noise arising from low-dose scan settings and image artifacts arising from the X-ray cone-beam geometry and rapid circulation of contrast in the heart chambers [2–4]. We have previously validated the effectiveness of a whole-heart coverage CT system for minimizing image noise and artifacts for CT myocardial perfusion measurement [5]. In this paper, we investigated the diagnostic accuracy of CTP for assessing functionally significant coronary artery

stenosis in patients with known (stable) or suspected CAD using this CT system.

2. Methods

2.1. Patient preparation

The study was conducted at Kaohsiung Veteran General Hospital from January 2016 to February 2017, and was approved by the institution ethics review committee. Symptomatic patients with suspected or known CAD who were referred for functional assessment of MBF as part of the standard-of-care procedure were screened. Patients with the following conditions were excluded from the study: pregnancy, previous coronary bypass surgery, acute coronary syndrome, second- or third- degree of AV block without pacemaker, atrial fibrillation, allergy contraindication to iodinated contrast medium and/or vasodilator, active asthma, renal insufficiency (estimated GFR ≤ 35 mL/min/m²), or inability to follow instruction. Twenty six patients (age 59.0 ± 8.0 years) who met the inclusion criteria and provided written informed consents were enrolled into the study. Each patient underwent both Single Photon Emission Computed Tomography (SPECT) myocardial perfusion imaging (MPI) with either Thallium-201 (Tl) or Technetium-99 m sestamibi (MIBI) tracers and CT MPI within 6 weeks. Neither percutaneous coronary intervention nor surgical revascularization was performed between the SPECT and CT MPI studies.

2.2. Cardiac CT studies

2.2.1. Patient preparation

An 18-gauge needle was inserted into the right antecubital vein for contrast administration and a 22-gauge needle was inserted into the left antecubital vein for dipyridamole administration. Neither beta-blocker nor nitroglycerin was used before imaging. Heart rate, blood pressure, and electrocardiogram (ECG) were monitored throughout the cardiac CT study.

2.2.2. Imaging protocol

Each CT study consisted of coronary CT angiography (CCTA), rest and stress CT MPI scans acquired with a 160-mm/256-row Revolution CT scanner (GE Healthcare Waukesha, WI). Fig. 1a illustrates the CT imaging protocol. There was a 10 min waiting period between rest and stress CT MPI scans to allow sufficient time for contrast to wash out of the myocardium. All CT acquisitions were performed with breath-holding.

2.2.3. CCTA

A scout image was first acquired to select image slices for CCTA. A bolus of iodinated contrast (Omnipaque 350, GE Healthcare) was then injected into the right antecubital vein at 5 ml/s injection rate and 0.8 ml/kg dosage, followed by 30 ml of saline flash at the same injection rate. A prospective electrocardiogram (ECG) gated axial scan of the whole heart was acquired after contrast enhancement in the ascending

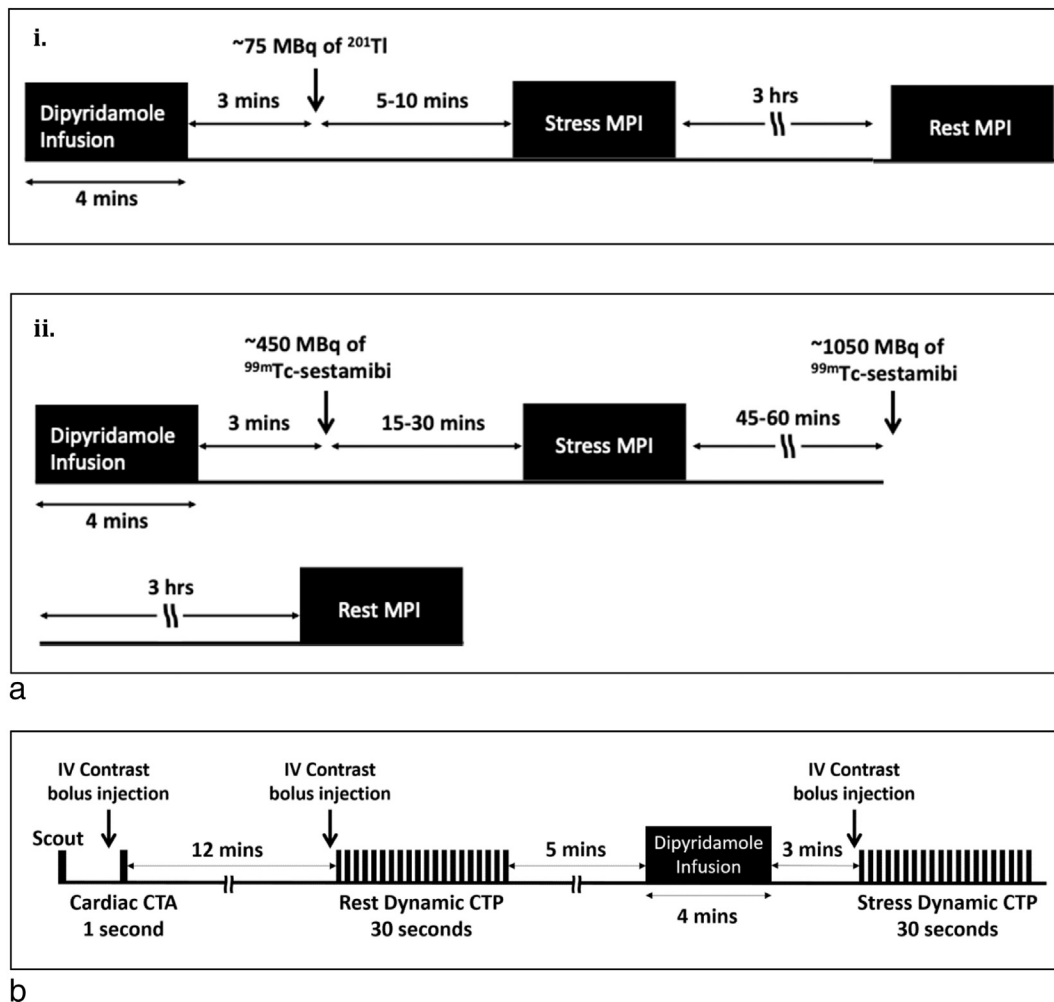Fig. 1. a. Protocol for rest and stress SPECT MPI with either (i) 201-Thallium or (ii) 99mTc-sestamibi tracers. b. Protocol for CCTA and dynamic rest and stress CT MPI. Each black bar represents a prospective ECG triggered axial scan of the heart.

aorta as monitored by a bolus tracking technique (Smart Prep) exceeded 150 HU. The scan settings used for CCTA were 100 kV (tube voltage), modulated mA (tube current) based on noise index of 30, and 280 ms gantry rotation period. After the acquisition, transaxial images were reconstructed with 0.625 mm slice thickness using a medium-to-smooth convolution kernel. If severe coronary artery calcification was present, an additional set of transaxial images was reconstructed with a sharp convolution kernel to reduce the partial volume effect. Diagnostic image quality of the CCTA images was graded by experienced radiologists using a 5-point scale ranging from 1 (worst) to 5 (best) according to published guidelines [6–7].

2.2.4. CT MPI

Rest CT MPI was performed at 10 min after the CCTA acquisition. A bolus of iodinated contrast was injected at 5 ml/s and 0.7 ml/kg into the right antecubital vein, followed by 30 ml of saline flash at the same injection rate. At about 5 s after contrast injection, prospective ECG gated scanning of the heart was performed using a dynamic acquisition protocol: 20 axial scans at mid-to-end diastole every 1 to 2 heart beats (heart rate dependent), 100 kV tube voltage, 100 mA tube current, 280 ms gantry rotation speed and 12 cm axial coverage. About 10 min after the rest CT MPI was completed, 0.56 mg/kg of dipyridamole (Persantine) was infused at a constant rate into the left antecubital vein over 4 min. CT MPI was repeated at 3 min after the completion of dipyridamole infusion with identical imaging and contrast injection protocols as for the rest CT MPI study. Aminophylline (50–100 mg) if required was administered at the end of the stress CT MPI study by an attending physician to relieve chest discomfort.

2.2.5. Generation of myocardial blood flow map

Dynamic contrast-enhanced (DCE) images of each CT MPI study were reconstructed at 2.5 mm slice thickness using the medium-smooth kernel, with correction of beam hardening, partial-scan and cone-beam artifacts using 100% adaptive statistical iteration reconstruction (ASiR, GE Healthcare) [5]. A proprietary three-dimensional non-rigid image registration algorithm (GE Healthcare) was used to minimize the misalignment of DCE images arising from residual cardiac and respiratory motion. The registered DCE images were reformatted into the short-axis view and thickened to 5 mm, before being analyzed with the CT Perfusion software (GE Healthcare) to generate MBF maps. This software applies a model-based deconvolution algorithm to derive absolute myocardial blood flow based on the temporal changes of contrast enhancement in tissue and blood during a short dynamic imaging session [8]. Unlike the compartmental model, the distributed parameter model of the intra- and extra-vascular spaces whereby the deconvolution is constrained allows blood flow and vascular extraction efficiency to be modeled independently from the measured arterial and myocardial time-enhancement curves [9]. After MBP maps of the rest and stress studies were generated, MPR was calculated as the ratio of the stress MBF to rest MBF in each short-axis myocardial segment.

2.3. SPECT MPI

SPECT MPI was performed with a SPECT/CT imaging system (Symbia S or E system, Siemens Healthineers, Erlangen, Germany) using a routine one-day stress-rest protocol [10,11] with either the ^{99m}Tc-sestamibi tracers at an average dose of 1500 MBq or the Thalium-201 (^{201}Tl) tracers at an average dose of 75 MBq. In all the stress MPI studies, the perfusion tracers were administered at 3 min after a 4-minute constant infusion of dipyridamole at 0.56 mg/kg. For ^{201}Tl SPECT, stress MPI commenced at 5–10 min after tracer injection and rest MPI began at 3 h later. For ^{99m}Tc-sestamibi SPECT, stress MPI commenced at 15–30 min after tracer injection followed by a 3-hour waiting period. Another dose of tracer injection was then administered and rest MPI began at 45–60 min later (Fig. 1b).

All SPECT cardiac images were reformatted into the three orthogonal views for analysis. The QPS software (Cedars-Sinai Medical Center, Los Angeles, CA) was used to generate SPECT MBF polar maps according to the American Heart Association (AHA) 17 short-axis segment model, which were evaluated by an experienced Nuclear Medicine physician according to the criteria defined by the ACC/AHA/ACP-ASIM guidelines. Perfusion in each myocardial segment was qualitatively assessed using a 5-point scoring system: 0 = normal, 1 = mild reduction, 2 = moderate reduction, 3 = severe reduction, 4 = absence. A myocardial segment was defined as ischemic if the segmental score was greater than or equalled to 2.

2.4. Invasive coronary angiography

Patients who had evidence of myocardial ischemia by the SPECT MPI test were further investigated with invasive (catheter-based) coronary angiography (ICA) performed according to routine clinical guidelines. The degree of stenosis in each coronary artery was assessed as percentage of luminal narrowing using the CAAS II system (Pie Medical, Maastricht, the Netherlands).

2.5. Data analysis

2.5.1. Definition of functionally significant CAD

Functionally significant CAD was defined as one of the following criteria: (1) ≥70% narrowing in a major coronary artery and/or ≥50% narrowing in the left main artery; (2) 50–69% narrowing in a major coronary artery with downstream ischemia assessed by SPECT; (3) Culprit lesions of previous episode of ST-elevated myocardial infarction (STEMI) or non STEMI. CCTA was used as the alternative reference standard of coronary patency only if ICA was not performed within 6 weeks before or after the CT MPI study. The conjunctional use of ICA and SPECT MPI as reference standard is justified by the fact that SPECT MPI has moderate specificity [12] and ICA can reduce the number of false positive cases due to artifacts arising from breast, diaphragm and/or chest wall, and the number of false negative cases due to balanced ischemia when only SPECT MPI is used.

2.5.2. Assignment of coronary territories

The assignment of coronary territories on the CT and SPECT myocardial perfusion maps was based on the AHA 17 segment model for short-axis tomographic plane. The segment at the apex (17th segment) in all patients was excluded for analysis because of significant movement. Adjustment of coronary territory assignment was made if necessary to address individual variation in the coronary anatomy based on the CCTA images. The dominance of coronary system was also assessed with either the ICA or CCTA images. If there were multiple functionally significant lesions in a coronary artery, the one closest to the orifice was considered as the major lesion and all the downstream myocardial segments were classified as ischemic. On the contrary, all the myocardial segments above a functionally significant lesion were classified as non-ischemic.

2.5.3. Statistical analysis

A binomial logistic regression analysis was used to identify predictors of functionally significant coronary stenosis. Receiver operating characteristic (ROC) curve analysis was used to assess the discriminatory power of the stress MBF and MPR measurements for differentiating ischemic from non-ischemic myocardial segments, expressed as the area under the curve (AUC) and its 95% confident intervals (CI). Optimal cut-off values for stress MBF and MPR were defined as the values that led to maximization of the Youden index J, where J = sensitivity + specificity − 1.

All the statistical tests were performed using the SPSS software for Windows (version 18.0, IBM Corp., Armonk, NY) and the MedCalc software (version 17.5.3, MedCalc Software, Ostend, Belgium). For all the

statistical tests, a p value < 0.05 was considered as statistically significant.

The sensitivity, specificity, positive predictive value (PPV), negative predictive value (NPV), and diagnostic accuracy of stress MBF, MPR and combined stress MBF and MPR (sMBF+MPR) for detection of functionally significant CAD were evaluated using the per-patient, per-vessel and per-segment analysis. sMBF+MPR refers to the concomitant use of both parameters for CAD classification based on their respective optimal thresholds determined from the Youden indexes described above. In the vessel-based analysis, the supplying artery of a coronary territory was considered as functionally significant if the coronary territory had one or more ischemic myocardial segments within it. In the patient-based analysis, the patient was considered to have a functionally significant CAD if he/she had one or more functionally stenosed coronary arteries.

The incremental diagnostic value of CTP to CCTA for identifying functionally significant CAD was also investigated. The diagnostic accuracy of CCTA and combined CCTA and CTP (CCTA+CTP) were determined against ICA and SPECT MPI using the same criteria defined in Section 2.5.1. Two thresholds were used to define a positive CCTA finding: ≥50% or ≥70% narrowing in a major coronary artery. The CTP result was considered as positive if both sMBF and MPR were below their cut-off thresholds determined from the Youden index as discussed in this section.

3. Results

3.1. Patients

Twenty-six patients completed both SPECT and CT MPI within 6 weeks after the recruitment. Five patients were excluded for perfusion analysis because the baseline (non-enhanced phase) of the time-enhancement curves was not captured in the CT MPI study due to mistiming of the start of the dynamic acquisition. The remaining 21 patients had a total of 336 short-axis myocardial segments, but 11 of those segments were excluded for analysis due to severe motion (n = 9) and post-infarct wall thinning (n = 2, <3 mm thickness), leaving a total of 325 short-axis myocardial segments for analysis.

Of the 21 patients included for analysis, 18 had ICA performed within 6 weeks after CT MPI. For the other three patients, CCTA was used to evaluate the percentage of lumen narrowing in each coronary artery. All the CCTA images had good image quality (mean score 3.7 ± 0.6) for anatomical assessment of CAD. The subgroup analysis on the incremental value of CTP to CCTA was performed on the 18 patients who had ICA acquired within 6 weeks of CT MPI.

The mean heart rates of the CCTA and rest CT MPI studies were 69.5 ± 8.9 and 67.2 ± 8.6 beats per minute (bpm), respectively. Upon the completion of 4-minute infusion of dipyridamole prior to the stress CT MPI, the mean heart rate increased to 88.6 ± 11.1 bpm.

Functionally significant CAD was diagnosed in 15 patients according to the criteria described in Section 2.5.1, including single-vessel (n = 8), double-vessel (n = 5), and triple-vessel (n = 2) diseases (Table 1). On a per-vessel analysis, functionally significant lesions were found in 24 coronary arteries: 4 in the right coronary artery (RCA), 10 in the left anterior descending artery (LAD), 10 in the left circumflex artery (LCX), and none in the left main artery (LM). Coronary stents were found in 17 coronary arteries: 3 in the RCA, 10 in the LAD, and 4 in the LCX. Previous myocardial infarcts were found in 7 patients, including 4 non-STEMI (2 in the LAD and 2 in the LCX territories) and 3 STEMI (2 in the LAD and 1 in the RCA territories) (Fig. 2).

3.2. Mean MBF and MPR in ischemic and non-ischemic myocardium

There were a total of 230 (70.8%) non-ischemic and 95 (29.2%) ischemic myocardial segments available for analysis. The mean rest MBF values between the non-ischemic (0.87 ± 0.24 ml/min/g) and ischemic

Table 1
Summary of patient characteristics. Except for the physical measurements, the numbers in the table represent the number of patients and the numbers in the bracket denote the percentage of patients.

Number of patient	21
Male/female	18/3
Age (years)	59.0 ± 8.0
Body mass index (kg/m^2)	24.8 ± 2.4
Height (cm)	164.8 ± 8.5
Weight (kg)	67.5 ± 8.8
Coronary dominance	
Right	18 (86%)
Left	2 (10%)
Co	1 (4%)
Cardiovascular risk factors	
Hypertension	10 (48%)
Dyslipidemia	9 (43%)
Diabetes	5 (24%)
Family history of CAD	1 (5%)
Smoking within the last year	6 (29%)
CAD	
Single-vessel disease	8 (38%)
Double-vessel disease	5 (24%)
Triple-vessel disease	2 (10%)
Prior myocardial infarction	7 (33%)
Prior PCI	12 (57%)
Prior Stent	12 (57%)
Agatston coronary calcium score	346.2 ± 412.1
MESA risk score	82.3 ± 17.8

(0.90 ± 0.16 ml/min/g) groups were not statistically different from each other (p > 0.05, Fig. 3a). However, the mean stress MBF value in the ischemic segments (1.37 ± 0.34 ml/min/g) was significantly lower than that in the non-ischemic segments (2.14 ± 0.64 ml/min/g, p < 0.05, Fig. 3a). Consequently, the mean MPR value in the ischemic segments (1.56 ± 0.41) was significantly lower than that in the non-ischemic segments (2.53 ± 0.70, p < 0.05, Fig. 3b).

The scatterplot of the MPR values against the corresponding stress MBF values for all the myocardial segments is shown in Fig. 4a. The measurements acquired from the non-ischemic myocardial segments (green triangles) were more clustered in the upper right quadrant of the graph whereas those acquired from the ischemic segments (blue circles) were mainly located in the lower left quadrant of the graph.

3.3. Logistic regression and ROC analysis

The binomial logistic regression model identified both MPR and stress MBF as significant predictors of the functionally significant coronary stenosis. The ROC analysis (Fig. 4b) showed that MPR (AUC 0.916, 95%CI: 0.885–0.947) had a superior power than stress MBF (AUC 0.869, 95%CI: 0.830–0.909) for differentiating non-ischemic and ischemic myocardial segments (p = 0.045). With an optimal cut-off threshold of 2.0 as determined from the Youden index, MPR had a 87.4% sensitivity (95%CI: 78.97%–93.30%), 82.2% specificity (95%CI: 76.60%–86.89%), 66.9% positive predictive value (PPV, 95% CI: 60.29%–72.97%), and 94.0% negative predictive value (NPV, 95% CI: 90.24%–96.41%) on a segment-based analysis (Table 2). With an optimal cut-off threshold of 1.60 ml/min/g, stress MBF had a sensitivity, specificity, PPV and NPV of 81.1% (95%CI: 71.72%–88.37%), 83.9% (95%CI: 78.51%–88.41%), 67.5% (95%CI: 60.40%–73.96%), and 91.5% (95%CI: 87.57%–94.22%), respectively, on a segment-based analysis (Table 2). The concomitant use of stress MBF and MPR thresholds (stress MBF < 1.6 mL/g/min and MPR < 2.0) improved the specificity and PPV compared to either stress MBF or MPR alone on all the three analysis methods, and improved the overall diagnostic accuracy compared to stress MBF or MPR alone on the vessel- and segment-based analysis methods.
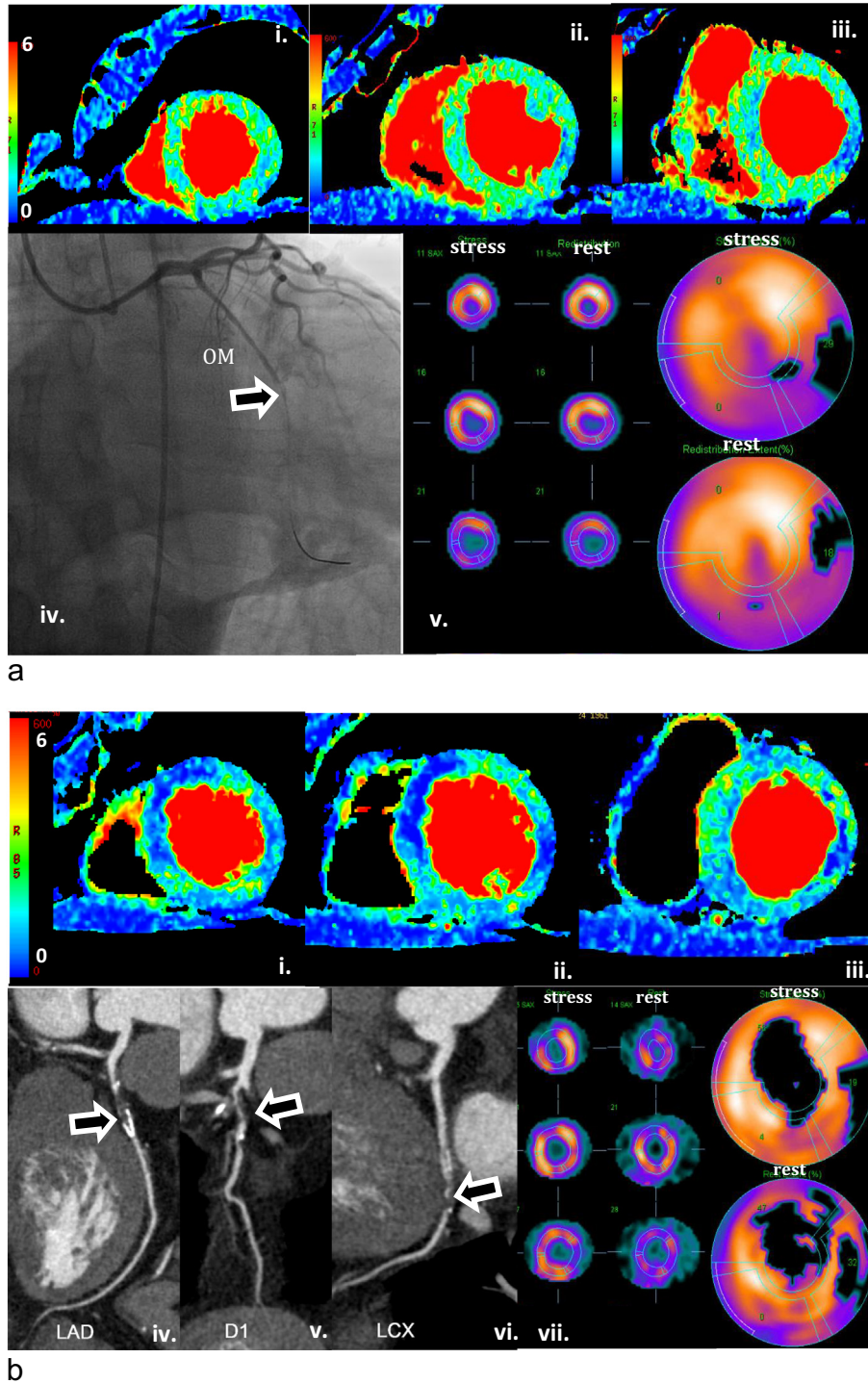
Fig. 2. a. This figure shows the case of a 55 y.o. male patient who had a positive treadmill test. The ICA test revealed that he had a single-vessel CAD with a totally occluded obtuse marginal branch (black arrow in iv). The SPECT perfusion maps in the short-axis and polar view revealed a perfusion defect in the basal and mid lateral wall (LCx territory, v). The CT stress perfusion maps in three short-axis slices (i to iii) also revealed ischemia in the lateral wall in the basal and mid slices. b. This figure shows the case of a different 55 y.o. male patient who had exertional chest pain during exercise and was diabetic with a double-vessel CAD. The CCTA images showed that the proximal LAD segment was sub-totally occluded and the proximal LCx segment was 90% stenosed (black arrows in iv to vi), whereas the RCA artery was non-stenosed. The SPECT perfusion maps in the short-axis and polar view (vii) showed profound hypoperfusion in the lateral wall (LCx territory) and apical wall (LAD territory). The CT stress perfusion maps in three short-axis slices (i to iii) also showed intense hypoperfusion in approximately the same lateral and apical myocardial segments. c. This figure shows the case of a 59 y.o. male patient who had a triple-vessel CAD and unstable angina. He had a prior myocardial infarction (non-STEMI) and a stent was implanted in the proximal LAD artery about 17 months before his enrolment for this study. The ICA showed that the proximal and mid RCA segments were 70% and 99% stenosed respectively (black arrows in iv); the mid LAD segment was 60% stenosed, with additional 80% and 70% stenosis in the first and second diagonal branches respectively (black arrows in v); the distal LCx segment was totally occluded. The SPECT perfusion maps in the short-axis and polar view (vi) showed absence of or minimal hypoperfusion due to the "balanced" ischemia commonly seen in multi-vessel CAD. By contrast, the CT stress perfusion maps in three short-axis slices (i to iii) clearly showed ischemia in all three coronary territories.
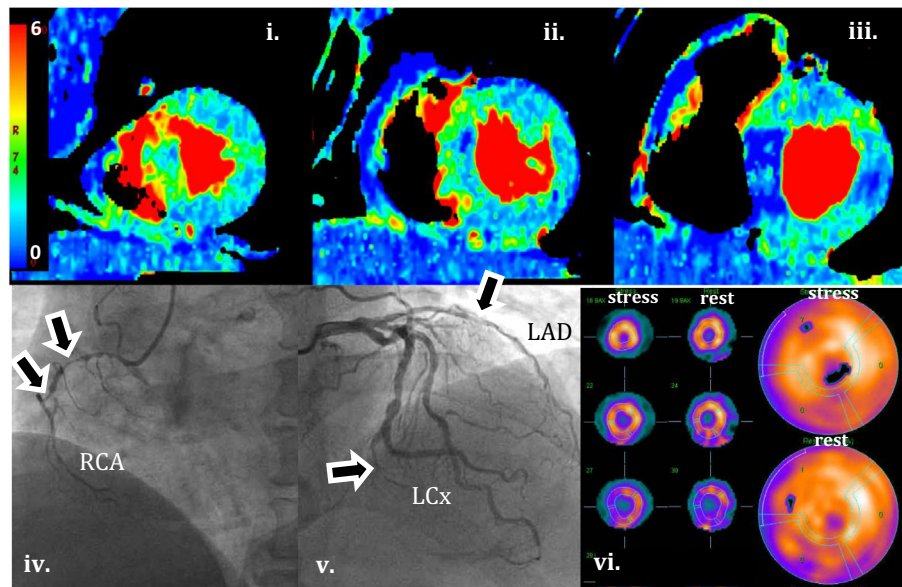
Fig. 2 (*continued*).

3.4. Incremental value of CTP to CCTA

The diagnostic performances of CCTA and CCTA+CTP in detecting functionally significant coronary artery stenosis are summarized in Table 3. Per-vessel and per-patient analyses showed that the accuracy of CCTA was 71.2% and 77.8%, respectively. Both analyses revealed no difference in the accuracy of CCTA between the ≥50% or ≥70% narrowing thresholds. When CTP was used in conjunction with CCTA (i.e. CCTA +CTP), the accuracy increased to 92.3% and 100% on per-vessel and per-patient analyses respectively. Furthermore, the sensitivity and NPV of CCTA+CTP were higher than those of CCTA or CTP alone on both per-vessel and per-patient analyses.

3.5. Effective doses

The average dose-length product (DLP) of the CCTA, rest CT MPI and stress CT MPI studies reported from the Revolution CT scanner console were 123.4, 217.48 and 227.70 mGy·cm respectively. The projected effective doses of these studies were 1.73, 3.04 and 3.19 mSv respectively.

4. Discussion

4.1. Comparison to other CT MPI studies

A number of diagnostic accuracy studies have been conducted in patients with stable CAD to determine the clinical feasibility of CT MPI for assessing obstructive coronary artery stenosis. Bamberg and colleagues [13] examined CT MPI against cardiac magnetic resonance imaging (CMR) in 31 patients with stable CAD and reported a sensitivity of 77.8% (95% CI, 69% to 85%) for detecting perfusion defects. Greif and colleagues [14] elevated the diagnostic accuracy of CT MPI against invasive fractional flow reserve measurement in 65 patients with suspected CAD. While CCTA alone had high sensitivity [15,16], the addition of CT MPI improved specificity and overall diagnostic accuracy (43.8% vs. 65.6% and 72% vs. 81.5%, respectively). Furthermore, a recent meta analysis conducted by Danad and colleague [17] revealed an average sensitivity of 88% and specificity of 71% for CT MPI in detecting functionally significant CAD against different reference techniques. The higher sensitivity (92% vs. 88%) and specificity (86% vs. 71%) shown in our findings (Table 2) could be contributed by the use of advanced technology for correcting various forms of image artifact and the use of a more realistic tracer kinetic model for describing the contrast exchange between blood and tissue for the deconvolution analysis. Compared to our previous single-center study conducted with an older 64-row CT scanner [18], the diagnostic accuracy of MPR for detecting obstructive coronary lesions improved from 78.5% to 83.6%, further highlighting the importance of advanced CT technology capable of minimizing the effect of cardiac motion and image artifacts.

Additionally, the present study shows higher stress perfusion values, in both normal and ischemic myocardium, compared to other recent dynamic CT MPI studies with absolute stress perfusion values reported. For instance, Ho and colleagues reported the global hyperemic MBF in ischemic myocardium in CAD patients to be 81.9 ± 18.5 ml/min/100 g [19]. Similarly, Bamberg and colleagues found the stress MBF in ischemic tissue was 72.7 ± 25.8 ml/min/100 g [13], which was in good agreement with that reported by Greif and colleagues (78.7 ± 26.1 ml/min/ 100 g) [14]. The differences in absolute MBF values could be attributed to the different analytic algorithms applied to estimate MBF. These studies used a two-compartment model of intra- and extra-vascular space to fit the measured time-enhancement curves with deconvolution, and MBF was estimated using the maximum slope of the fitted time-enhancement curves [20]. It has been shown in previous phantom simulation and patient studies [21,22] that this approach may result in a precise but significantly underestimated myocardial perfusion, as the estimated perfusion value is likely a product of MBF and vascular extraction efficiency, not solely MBF. Since the capillary permeability is different among different tissue physiological conditions [23,24], assuming a fixed value of vascular extraction efficiency to derive MBF with this approach may lead to different extents of underestimation of MBF in the normal, ischemic and infarcted myocardium, and consequently, a larger overlapping in stress MBF and MPR between them. This is evident in Bamberg's study where the stress MBF in ischemic and infarcted myocardial segments were identical to each other (72.3 ± 18.7 and 73.1 ± 31.9 ml/min/100 g, respectively) [13], and the indifferent MPR between the ischemic and infarcted groups as shown in Ho's study (1.33 ± 0.27 and 1.33 ± 0.46, respectively) [19].
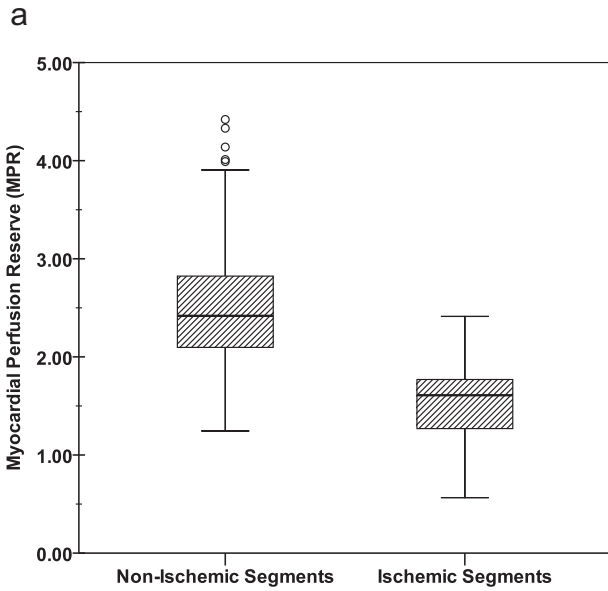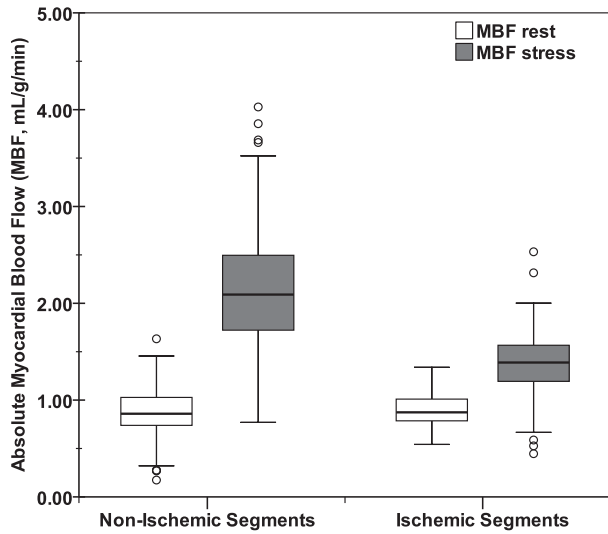
a

b

Fig. 3. a. Boxplot of rest and stress MBF in non-ischemic and ischemic myocardial segments. b. Boxplot of MPR in non-ischemic and ischemic myocardial segments.

a

b

Fig. 4. a. Scatter plot of MPR versus stress MBF for non-ischemic (green triangles) and ischemic (blue circles) myocardial segments. b. ROC curves of stress MBF (dot line) and MPR (solid bold line) for the detection of functionally significant CAD.

4.2. Comparison to PET MPI studies

Our findings also compared favourably to the previous findings by positron emission tomography (PET) which is the imaging gold standard for myocardial perfusion measurement. Gould and colleagues [1] examined over 5000 clinical PET MPI studies and concluded that the mean MPR value in the patients with CAD is 2.02 ± 0.70, which is considerably lower than that in the high-risk patients without CAD (2.80 ± 1.39). In comparison, our results revealed a similar difference in mean MPR value between the ischemic and non-ischemic groups: 1.56 ± 0.41 versus 2.53 ± 0.70 respectively.

It has been shown the usefulness of plotting coronary flow reserve against stress coronary flow for studying the coronary flow capacity under different hemodynamic conditions [25]. In this scatter plot, the PET MRI data resides in the upper right quadrant represents normal coronary flow capacity whereas the data resides in the lower left quadrant indicates impaired flow capacity. The scatter plot generated with our CT MPI data (Fig. 3a) was highly reminiscent of that with the PET MPI data shown by Gould and colleagues. Specifically, the data within the normal
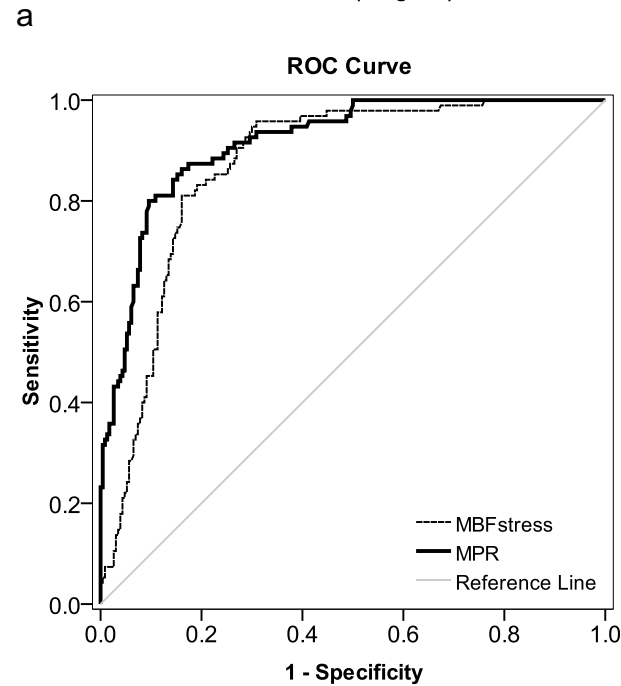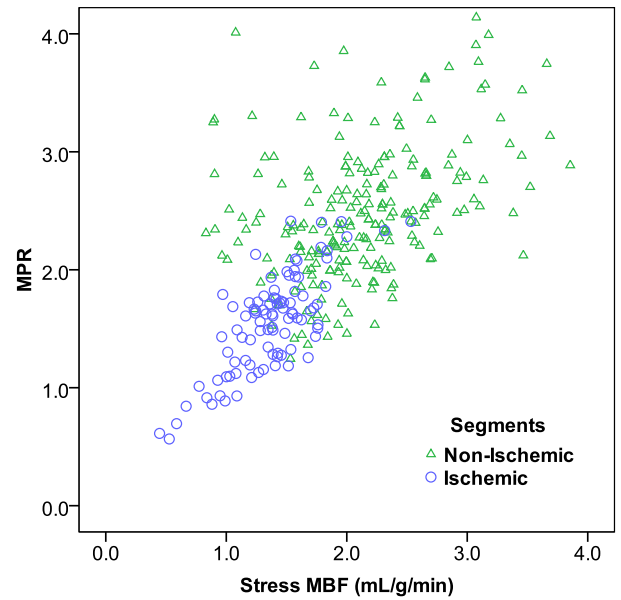
flow capacity zone was acquired from the non-ischemic myocardium whereas the data within the attenuated flow capacity zone was from the ischemic segments. Our results indicated that CTP could be an alternative to PET for functional assessment of CAD through quantitative measurement of myocardial perfusion.

4.3. Radiation dose

A recent meta-analysis on high-quality studies showed that the mean effective dose of a stress CT MPI study with a dynamic acquisition protocol was 9.23 mSv [17]. With the use of advanced image reconstruction algorithms for minimizing x-ray photon noise and beam hardening [5], we were able to perform CT MPI using a low kV/mA setting with an effective dose of 3.2 mSv only. Furthermore, in contrast to other

Table 2
Diagnostic performances of stress MBF (sMBF) and MPR and combined sMBF and MPR (sMBF+MPR) thresholds for detection of functionally significant coronary artery stenosis on a per-patient (top), per-vessel (middle) and per-segment (bottom) analysis.

Patient-based	sMBF			MPR			sMBF+MPR		
Parameter	Value	95% CI		Value	95% CI		Value	95% CI	
Sensitivity (%)	100.00	78.20 to 100.00		93.33	68.05 to 99.83		93.33	68.05 to 99.83	
Specificity (%)	83.33	35.88 to 99.58		66.67	22.28 to 95.67		100.00	54.07 to 100.00	
PPV (%)	93.75	71.48 to 98.90		87.50	69.13 to 95.63		100.00	–	
NPV (%)	100.00	–		80.00	35.66 to 96.65		85.71	47.46 to 97.55	
Accuracy (%)	95.24	76.18 to 99.88		85.71	63.66 to 96.95		95.24	76.18 to 99.88	
Vessel-based	sMBF			MPR			sMBF+MPR		
Parameter	Value	95 CI		Value	95 CI		Value	95 CI	
Sensitivity (%)	91.67	73.00 to 98.97		87.50	67.64 to 97.34		87.50	67.64 to 97.34	
Specificity (%)	86.49	71.23 to 95.46		81.08	64.84 to 92.04		97.30	85.84 to 99.93	
PPV (%)	81.48	65.87 to 90.93		75.00	60.22 to 85.60		95.45	75.12 to 99.32	
NPV (%)	94.12	80.84 to 98.38		90.91	77.43 to 96.68		92.31	80.61 to 97.19	
Accuracy (%)	88.52	77.78 to 95.26		83.61	71.91 to 91.85		93.44	84.05 to 98.18	
Segment-based	sMBF			MPR			sMBF+MPR		
Parameter	Value	95 CI		Value	95 CI		Value	95 CI	
Sensitivity (%)	81.05	71.72 to 88.37		87.37	78.97 to 93.30		76.84	67.06 to 84.88	
Specificity (%)	83.91	78.51 to 88.41		82.17	76.60 to 86.89		95.22	91.60 to 97.59	
PPV (%)	67.54	60.40 to 73.96		66.94	60.29 to 72.97		86.90	78.67 to 92.27	
NPV (%)	91.47	87.57 to 94.22		94.03	90.24 to 96.41		90.87	87.33 to 93.50	
Accuracy (%)	83.08	78.55 to 86.99		83.69	79.22 to 87.54		89.85	86.04 to 92.91	

dynamic acquisition protocols with comparable effective doses (for example the one employed by Kim and colleagues [26]), our dynamic imaging protocol offers a wider axial coverage (120 mm versus 73 mm) and a longer temporal coverage (30 s versus 14 s). The larger axial coverage of the heart allows assessment of lesion-specific ischemia with a single contrast bolus injection in cases of multiple stenoses within a coronary artery, while more dynamic (temporal) data available for the model-based deconvolution analysis may lead to a more accurate perfusion measurement.

4.4. Clinical implications

Our findings indicated that whole-heart quantitative myocardial perfusion measurement with a short bolus injection of contrast and low-dose dynamic CT acquisition session is clinically feasible. This rapid imaging technique may permit a more robust evaluation of functionally significant left main and multi-vessel CAD to facilitate triage for coronary revascularization [27–29], where the qualitative perfusion

Table 3
Diagnostic performances of CCTA and combined CCTA and CTP (CCTA+CTP) for detection of functionally significant coronary artery stenosis on a per-patient (top) and per-vessel (bottom) analysis.

Patient-based	Sensitivity (%)	Specificity (%)	PPV (%)	NPV (%)	ACCURACY (%)
CCTA ≥50%	92.86	25.00	81.25	50.00	77.78
CCTA ≥70%	71.43	100.00	100.00	50.00	77.78
sMBF	100.00	75.00	93.33	100.00	94.44
MPR	92.86	50.00	86.67	66.67	83.33
sMBF+MPR	92.86	100.00	100.00	80.00	94.44
CCTA+CTP[a]	100.00	100.00	100.00	100.00	100.00
Vessel-based	Sensitivity (%)	Specificity (%)	PPV (%)	NPV (%)	Accuracy (%)
CCTA ≥50%	65.22	75.86	68.18	73.33	71.15
CCTA ≥70%	43.48	93.10	83.33	67.50	71.15
sMBF	91.30	82.76	80.77	92.31	86.54
MPR	86.96	75.86	74.07	88.00	80.77
sMBF+MPR	86.96	96.55	95.24	90.32	92.31
CCTA+CTP[a]	95.65	89.66	88.00	96.30	92.31

[a] Both sMBF and MPR thresholds were used in the CCTA+CTP assessment.

assessment may become unreliable due to the presence of balanced ischemia. Compared to CCTA alone, CTP provided incremental diagnostic value for assessing obstructive coronary lesions identified by ICA or a combination of ICA and SPECT MPI. Our findings showed that the conjunctional use of CCTA and CTP resulted in a higher overall diagnostic accuracy by improving not only the sensitivity of detecting obstructive coronary lesions but also the ability of ruling them out. Our results also revealed that the combined use of stress MBF and MPR thresholds yielded a higher diagnostic accuracy for detecting functionally significant CAD compared to stress MBF alone. This finding is consistent with the notion that the functional significance of a coronary artery stenosis should be correlated to both the level of downstream perfusion at stress and the capability to elevate blood flow from baseline through dilation of the large epicardial coronary arteries and microcirculation [30].

4.5. Limitations

The CT MBF measurements were only compared to the qualitative SPECT data that was acquired from routine functional tests, and not to the clinical gold standard PET or CMR. While the quantitative CT MBF values were comparable with the quantitative PET MBF values reported in previous literatures, it would have been more compelling if a head-to-head comparison between absolute CT and PET perfusion measurements was conducted in the same study patients; Furthermore, we did not exclude patients that had prior myocardial infarction, which could have affected the correlation between CT measured MBF and coronary artery stenosis. However, these enrolled patients represent real-world symptomatic patients in whom a functional test is clinically indicated. Furthermore, a prior myocardial infarct may be distinguishable from functional ischemia by the fixed (irreversible) perfusion defect seen in both rest and stress perfusion measurements.

5. Conclusion

Coupled with large-coverage CT scanner and advanced image reconstruction and processing techniques, quantitative CTP assessment of the whole heart with a low-dose imaging protocol is feasible and can evaluate the functional significance of coronary artery stenosis in symptomatic patients with a high diagnostic accuracy. The concomitant use of the

sMBF and MPR thresholds may yield the highest diagnostic accuracy for identifying obstructive coronary lesions. CTP also enhances the capability of cardiac CT by providing incremental diagnostic value to CCTA to enable a comprehensive anatomical and functional assessment of CAD in a single non-invasive test. A larger prospective multi-center study is warranted to further examine the diagnostic accuracy and clinical embracement of CTP for the evaluation of myocardial ischemia in patients with CAD.

Declaration of Competing Interest

T-Y Lee has a licensing agreement with GE Healthcare on the CT Perfusion software. Other authors report on conflict of interest.

Acknowledgement

References

[1] K.L. Gould, N.P. Johnson, T.M. Bateman, et al., Anatomic versus physiologic assessment of coronary artery disease. Role of coronary flow reserve, fractional flow reserve, and positron emission tomography imaging in revascularization decision making, J. Am. Coll. Cardiol. 62 (18) (2013) 1639–1653.
[2] R.A. Brooks, G. Di Chiro, Beam hardening in x-ray reconstructive tomography, Phys. Med. Biol. 21 (1976) 390–398.
[3] K. Taguchi, J. Cammin, A new redundancy weighting scheme for nonstationary data for computed tomography, Med. Phys. 42 (5) (2015) 2659–2667.
[4] A. Katsevich, A general scheme for constructing inversion algorithms for cone beam CT, Int. J. Math. Sci. 21 (2003) 1305–1321.
[5] A. So, Y. Imai, B. Nett, et al., Technical note: evaluation of a 160-mm/256-row CT scanner for whole-heart quantitative myocardial perfusion imaging, Med. Phys. 43 (8) (2016 Aug) 4821.
[6] T.A. Fuch, J. Stehli, M. Fiechter, et al., First experience with monochromatic coronary computed tomography angiography from a 64-slice CT scanner with Gemstone Spectral Imaging (GSI), J. Cardiovasc. Comput. Tomogr. 7 (1) (2013) 25–31.
[7] J. Leipsic, T.M. Labounty, B. Heilbron, et al., Adaptive statistical iterative reconstruction: assessment of image noise and image quality in coronary CT angiography, AJR Am. J. Roentgenol. 195 (3) (2010) 649–654.
[8] A. So, J. Hsieh, J.Y. Li, et al., Quantitative myocardial perfusion measurement using CT perfusion: a validation study in a porcine model of reperfused acute myocardial infarction, Int. J. Cardiovasc. Imaging 28 (5) (2012) 1237–1248.
[9] K.S. St Lawrence, T.Y. Lee, An adiabatic approximation to the tissue homogeneity model for water exchange in the brain: I. Theoretical derivation, J. Cereb. Blood Flow Metab. 18 (12) (1998) 1365–1377.
[10] B. Hesse, K. Tagil, A. Cuocolo, et al., EANM/ESC procedural guidelines for myocardial perfusion imaging in nuclear cardiology, Eur. J. Nucl. Med. Mol. Imaging 32 (7) (2005) 855–897.
[11] H.W. Strauss, D.D. Miller, M.D. Wittry, et al., Procedure guideline for myocardial perfusion imaging 3.3, J. Nucl. Med. Technol. 36 (3) (2008) 155–161.
[12] C. Kim, Y.S. Kwok, P. Heagerty, et al., Pharmacologic stress testing for coronary disease diagnosis: a meta-analysis, Am. Heart J. 142 (6) (2001) 934–944.
[13] F. Bamberg, R. Hinkel, F. Schwarz, et al., Accuracy of dynamic computed tomography adenosine stress myocardial perfusion imaging in estimating myocardial blood flow at various degrees of coronary artery stenosis using a porcine animal model, Investig. Radiol. 47 (2012) 71–77.
[14] M. Greif, F. von Ziegler, F. Bamberg, et al., CT stress perfusion imaging for detection of haemodynamically relevant coronary stenosis as defined by FFR, Heart. 99 (2013) 1004–1011.
[15] J.M. Miller, C.E. Rochitte, M. Dewey, et al., Diagnostic performance of coronary angiography by 64-row CT, N. Engl. J. Med. 359 (22) (2008) 2324–2336.
[16] W.B. Meijboom, M.F. Meijs, J.D. Schuijf, et al., Diagnostic accuracy of 64-slice computed tomography coronary angiography: a prospective, multicenter, multivendor study, J. Am. Coll. Cardiol. 52 (25) (2008) 2135–2144.
[17] I. Danad, J. Szymonifka, J. Schulman-Marcus, J.K. Min, Static and dynamic assessment of myocardial perfusion by computed tomography, Eur. Heart J. Cardiovasc. Imaging 17 (8) (2016 Aug) 836–844.
[18] A. So, G. Wisenberg, A. Islam, et al., Non-invasive assessment of functionally relevant coronary artery stenoses with quantitative CT perfusion: preliminary clinical experiences, Eur. Radiol. 22 (1) (2012 Jan) 39–50.
[19] K.T. Ho, H.Y. Ong, G. Tan, et al., Dynamic CT myocardial perfusion measurements of resting and hyperaemic blood flow in low-risk subjects with 128-slice dual-source CT, Eur. Heart J. Cardiovasc. Imaging 16 (3) (2015) 300–306.
[20] R.T. George, M. Jerosch-Herold, C. Silva, et al., Quantification of myocardial perfusion using dynamic 64-detector computed tomography, Investig. Radiol. 42 (12) (2007) 815–822.
[21] M. Bindschadler, D. Modgil, K.R. Branch, et al., Comparison of blood flow models and acquisitions for quantitative myocardial perfusion estimation from dynamic CT, Phys. Med. Biol. 59 (7) (2014) 1533–1556.
[22] M. Ishida, K. Kitagawa, T. Ichihara, et al., Underestimation of myocardial blood flow by dynamic perfusion CT: explanations by two-compartment model analysis and limited temporal sampling of dynamic CT, J. Cardiovasc. Comput. Tomogr. 10 (3) (2016) 207–214.
[23] A.C. Lardo, M.A. Cordeiro, C. Silva, Contrast-enhanced multidetector computed tomography viability imaging after myocardial infarction: characterization of myocyte death, microvascular obstruction, and chronic scar, Circulation 113 (3) (2006) 394–404.
[24] X.Y. Zhu, E. Daghini, A.R. Chade, et al., Myocardial microvascular function during acute coronary artery stenosis: effect of hypertension and hypercholesterolaemia, Cardiovasc. Res. 83 (2) (2009) 371–380.
[25] N.P. Johnson, K.L. Gould, Integrating noninvasive absolute flow, coronary flow reserve, and ischemic thresholds into a comprehensive map of physiological severity, JACC Cardiovasc. Imaging 5 (4) (2012 Apr) 430–440.
[26] S.M. Kim, Y.N. Kim, Y.H. Choe, Adenosine-stress dynamic myocardial perfusion imaging using 128-slice dual-source CT: optimization of the CT protocol to reduce the radiation dose, Int. J. Cardiovasc. Imaging 29 (2013) 875–884.
[27] P.A.L. Tonino, B. De Bruyne, N.H.J. Pijls, et al., Fractional flow reserve versus angiography for guiding percutaneous coronary intervention, N. Engl. J. Med. 360 (3) (2009) 213–224.
[28] N.H. Pijls, W.F. Fearon, P.A. Tonino, et al., Fractional flow reserve versus angiography for guiding percutaneous coronary intervention in patients with multivessel coronary artery disease: 2-year follow-up of the FAME study, J. Am. Coll. Cardiol. 56 (3) (2010) 177–184.
[29] L.J. Shaw, D.S. Berman, D.J. Maron, et al., Optimal medical therapy with or without percutaneous coronary intervention to reduce ischemic burden: results from the COURAGE trial nuclear substudy, Circulation 117 (10) (2008) 1283–1291.
[30] V.R. Taqueti, R. Hachamovitch, V.L. Murthy, et al., Global coronary flow reserve is associated with adverse cardiovascular events independently of luminal angiographic severity and modifies the effect of early revascularization, Circulation 131 (1) (2015) 19–27.